Vol. 2 No. 2 ADVANCES IN ATMOSPHERIC SCIENCES May 1985

NUMERICAL EXPERIMENT OF SIX-LEVEL IMPLICIT PRIMITIVE MODEL

Liu Ruizhi (刘瑞芝)

Institute of Atmospheric Physics, Academia Sinica, Beijing

Received March 16, 1984

ABSTRACT

In this paper, a numerical test is carried out by using a six-level implicit primitive equation model defined in a π coordinate. The model equations are solved with nonlinear iterated method, yielding fairly good results.

However, it is time-consuming to solve the model with iterated method. Thus, this model is restored to the advective scheme and solved by means of a split method. Several actual examples are forecasted, which have yielded good results.

I. INTRODUCTION

The test on primitive equations was conducted in some countries during 1960s. At present, primitive equations are widely used to make numerical weather prediction, to study the general circulation of atmosphere and to simulate the climatic formation. We began this work from 1960s[1-2]. Zeng et al. designed a six-level implicit primitive model which obeys the rule of energy conservation[3]. In 1976 Zhu et al.[4] designed an explicit primitive model which obeys the rule of instantaneous energy conservation.

It is well known that the basic governing equations used in every primitive equation model are the same, but the treatments are different from each other. The primitive equation model is more complex than the quasi-geostrophic systems. They are very sensitive to the initial and boundary conditions and the finite difference scheme. In order to obtain satisfactory results, the finite difference equations, boundary conditions and initial conditions must be treated carefully, otherwise, they will generate computational instabilities. So it is a hard work to get a good result using the primitive equations.

In order to further improve the accuracy of numerical forecast, to simulate the general circulation of atmosphere and to study the problems of climatic formation, we should first suggest an available numerical forecast model. We constitute a six-level implicit primitive model, based on that designed by Zeng during 1960s. This model is shown in a π coordinate, $\pi=f(\zeta)$ with $\zeta=\dfrac{p-p_t}{p_s-p_t}$, where p, p_s and p_t are the pressures at arbitrary level, at the surface and at the highest level, respectively. The interval $\delta\pi$ between any two adjacent levels of normal atmosphere is equal.

In this model, all variables are written on the same π levels, so that the surface is also a forecast one. It is different from other models designed so far both at home and abroad.

In other models, the variables are on the integral levels and 1/2 levels, so the surface is not a forecast level. However, it is of practical value in forecasting all the meteorological elements of the surface level immediately. Therefore, we try to do it and study its forecast effect.

In order to properly describe the vertical construction of the atmosphere there must be enough divisions in the vertical. However the more the levels, the more the computing amount. At present, the capacity of the electronic computer is not so great as to treat such a complex model in our country. Huang and Li have indicated that at least six parameters are needed to describe the vertical construction of the atmosphere[5]. Therefore we use six-level model in this paper.

II. NONLINEAR ITERATIONAL ADAPTABILITY DIFFERENCE SCHEME OF A SIX-LEVEL IMPLICIT PRIMITIVE EQUATION (MODEL 1)

1. *Finite Difference Equations*

With the quasi-static approximation, the difference scheme of a six-level primitive equations written in a π coordintate is as follows:

$$\left(\frac{\delta_t^+ P^*_{es} u}{\delta t}\right)_{i,j,k} + \alpha D_{i,j,k}(\mathbf{w}^*\bar{u}) = \beta(-\bar{P}^*_{es}\bar{G}^{**}_x + \bar{\bar{f}}^*\bar{P}^*_{es}\bar{v}^{**})_{i,j,k} + Fu, \tag{1}$$

$$\left(\frac{\delta_t^+ P^*_{es} v}{\delta t}\right)_{i,j,k} + \alpha D_{i,j,k}(\mathbf{w}^*\bar{v}) = \beta(-\bar{P}^*_{es}\bar{G}^{**}_y - \bar{\bar{f}}^*\bar{P}^*_{es}\bar{u}^{**})_{i,j,k} + Fv, \tag{2}$$

$$\begin{aligned}\left(\frac{\delta_t^+ c_p P^*_{es} T}{\delta t}\right)_{i,j,k} &+ D_{i,j,k}(\mathbf{w}^*[\alpha c_p \bar{T}^* + \beta\bar{\phi}^{**}]) \\ &= \beta\Big[-\pi'\left(\frac{\partial \pi \xi \bar{\Phi}^{**}}{\delta \pi}\right)\left(\kappa \frac{\delta_t^+ P^*_{es}}{\delta_t}\right) + (\bar{P}^*_{es}\bar{G}^{**}_x \bar{u}^{**} \\ &\quad + \bar{P}^*_{es}\bar{G}^{**}_y \bar{v}^{**})\Big]_{i,j,k} + F_T,\end{aligned} \tag{3}$$

$$\kappa\left(\frac{\delta_t^+ P^*_{es}}{\delta t}\right)_{i,j} = -\sum_{k=1}^{K} \varepsilon_k \left(\frac{1}{\pi'}\right)_k \delta\pi (MN)_{i,j}\left[\frac{\delta_x U^*}{\delta x} + \frac{\delta_y V^*}{\delta y}\right]_{i,j,k}, \tag{4}$$

$$\begin{aligned} w^*_{i,j,k+1} - w^*_{i,j,k} = -\left(\frac{\delta\pi}{\pi'}\right)_{k+\frac{1}{2}} &\Big\{\kappa\left(\frac{\delta_t^+ P^*_{es}}{\delta t}\right)_{i,j} + \frac{1}{2}(MN)_{i,j} \\ &\times\Big[\left(\frac{\delta_x \tilde{U}^*}{\delta x} + \frac{\delta_y \tilde{V}^*}{\delta y}\right)_{i,j,k+1} + \left(\frac{\delta_x \tilde{U}^*}{\delta x} + \frac{\delta_y \tilde{V}^*}{\delta_y}\right)_{i,j,k}\Big]\Big\},\end{aligned} \tag{5}$$

$$\phi_{i,j,k-1} - \phi_{i,j,k} = \frac{R}{2}[(T)_{i,j,k} + (T)_{i,j,k-1}]\ln\left(\frac{\zeta_k + P_t/P_{es}}{\zeta_{k-1} + P_t/P_s}\right)_{i,j}. \tag{6}$$

The notations $D_{i,j,k}(\mathbf{w}^*\bar{u})$, $D_{i,j,k}(\mathbf{w}^*\bar{v})$ and $D_{i,j,k}(\mathbf{w}^*[\alpha c_p \bar{T}^* + \beta\bar{\phi}^{**}])$ in Eqs. (1)— (3) are all expressed in terms of $D_{i,j,k}(\mathbf{w}^*\bar{F})$, which is given by:

$$D_{i,j,k}(\mathbf{w}^*\bar{F}) = (MN)_{i,j}\left[\frac{\partial_x U^*\bar{F}}{\delta x} + \frac{\partial_y V^*\bar{F}}{\delta y}\right]_{i,j,k} + \pi'_k\left(\frac{\partial_\pi w^*\bar{F}}{\delta \pi}\right)_{i,j,k} \tag{7}$$

$$\begin{cases} \bar{G}_x^{**}=M_{i,j}\left(\dfrac{\delta\bar{\Phi}^{**}}{\delta x}+\dfrac{R\bar{T}_e^{**}}{\bar{P}_{es}^{*}}\cdot\dfrac{\delta\bar{P}_{es}^{*}}{\delta x}\right) \\ \bar{G}_y^{**}=N_{i,j}\left(\dfrac{\delta\bar{\Phi}^{**}}{\delta y}+\dfrac{R\bar{T}_e^{**}}{\bar{P}_{es}^{*}}\cdot\dfrac{\delta\bar{P}_{es}^{*}}{\delta y}\right) \end{cases} \tag{8}$$

$$\bar{T}_e^{**}=\frac{\zeta}{\zeta+\dfrac{P_t}{P_{es}^{**}}}\bar{T}^{**}, \tag{9}$$

where $U^{*}_{i,j,k}$ and $V^{*}_{i,j,k}$ are the average values along the vertical direction, for example:

$$\begin{cases} U^{*}_{i,j,k}=\dfrac{1}{4}\left[\dfrac{\pi_k'}{\pi_{k+\frac{1}{2}}'}\bar{U}^{*}_{i,j,k+1}+2\bar{U}^{*}_{i,j,k}+\dfrac{\pi_k'}{\pi_{k-\frac{1}{2}}'}\bar{U}^{*}_{i,j,k-1}\right] \\ V^{*}_{i,j,k}=\dfrac{1}{4}\left[\dfrac{\pi_k'}{\pi_{k+\frac{1}{2}}'}\bar{V}^{*}_{i,j,k+1}+2\bar{V}^{*}_{i,j,k}+\dfrac{\pi_k'}{\pi_{k-\frac{1}{2}}'}\bar{V}^{*}_{i,j,k-1}\right], \end{cases} (k\neq 1,K), \tag{10}$$

$$\begin{cases} U^{*}_{i,j,0}=\dfrac{1}{2}(\bar{U}^{*}_{i,j,0}+\bar{U}^{*}_{i,j,1}) , \\ V^{*}_{i,j,0}=\dfrac{1}{2}(\bar{V}^{*}_{i,j,0}+\bar{V}^{*}_{i,j,1}) , \end{cases} \tag{11}$$

$$\begin{cases} U^{*}_{i,j,K}=\dfrac{1}{2}(\bar{U}^{*}_{i,j,K-1}+\bar{U}^{*}_{i,j,K}) , \\ V^{*}_{i,j,K}=\dfrac{1}{2}(\bar{V}^{*}_{i,j,K-1}+\bar{V}^{*}_{i,j,K}) . \end{cases} \tag{12}$$

$\bar{U}^{*}_{i,j,k}$ and $\bar{V}^{*}_{i,j,k}$ are the smooth terms of $\bar{u}$ and $\bar{v}$ in the horizontal area, i. e.

$$\begin{cases} \bar{U}^{*}_{i,j,k}=r'\left(\dfrac{\bar{P}^{*}_{es}\bar{u}}{N}\right)_{i,j,k}+(1-r')\dfrac{1}{4}\left[\left(\dfrac{\bar{P}^{*}_{es}\bar{u}}{N}\right)_{i+1,j,k}\right. \\ \qquad \left.+\left(\dfrac{\bar{P}^{*}_{es}\bar{u}}{N}\right)_{i-1,j,k}+\left(\dfrac{\bar{P}^{*}_{es}\bar{u}}{N}\right)_{i,j+1,k}+\left(\dfrac{\bar{P}^{*}_{es}\bar{u}}{N}\right)_{i,j-1,k}\right], \\ \bar{V}^{*}_{i,j,k}=r'\left(\dfrac{\bar{P}^{*}_{es}\bar{v}}{N}\right)_{i,j,k}+(1-r')\dfrac{1}{4}\left[\left(\dfrac{\bar{P}^{*}_{es}\bar{v}}{N}\right)_{i+1,j,k}\right. \\ \qquad \left.+\left(\dfrac{\bar{P}^{*}_{es}\bar{v}}{N}\right)_{i-1,j,k}+\left(\dfrac{\bar{P}^{*}_{es}\bar{v}}{N}\right)_{i,j+1,k}+\left(\dfrac{\bar{P}^{*}_{es}\bar{v}}{N}\right)_{i,j-1,k}\right], \end{cases} \tag{13}$$

$$\begin{cases} u^{*}_{i,j,k}=r'\times u_{i,j,k}+\dfrac{(1-r')}{4}(u_{i+1,j,k}+u_{i-1,j,k}+u_{i,j+1,k}+u_{i,j-1,k}), \\ v^{*}_{i,j,k}=r'\times v_{i,j,k}+\dfrac{(1-r')}{4}(v_{i+1,j,k}+v_{i-1,j,k}+v_{i,j+1,k}+v_{i,j-1,k}), \end{cases} \tag{14}$$

$$\begin{cases} u^{**}_{i,j,k}=r'\times u^{*}_{i,j,k}+\dfrac{(1-r')}{4}(u^{*}_{i+1,j,k}+u^{*}_{i-1,j,k}+u^{*}_{i,j+1,k}+u^{*}_{i,j-1,k}) , \\ v^{**}_{i,j,k}=r'\times v^{*}_{i,j,k}+\dfrac{(1-r')}{4}(v^{*}_{i+1,j,k}+v^{*}_{i-1,j,k}+v^{*}_{i,j+1,k}+v^{*}_{i,j-1,k}) , \end{cases} \tag{15}$$

Where $\bar{u}$ and $\bar{v}$ are time-average values.

P_t is the pressure at the atmospheric top and equals 100 hPa. P_s is the surface pressure. We have

$$p_{es}=p_s-p_t,$$
$$p_e=p-p_t,$$
$$\zeta=p_e/p_{es}.$$

M and N are the amplified coefficients of map projection along x and y directions, respectively. In the stereographic projection map, M and N are equal. F_u, F_v and F_r are friction terms along x, y and z, separately.

$$\tilde{\bar{f}}=f+u\frac{\partial N}{\partial y}-v\frac{\partial M}{\partial x}.$$

$\frac{\partial}{\partial x}$ and $\frac{\partial}{\partial y}$ represent central spacial difference within the area, and one-sided spacial difference on the boundary . They are all symbolized with $\frac{\delta}{\delta x}$ and $\frac{\delta}{\delta y}$.

$\frac{\partial}{\delta x}$ and $\frac{\partial}{\delta y}$ are presented as another central difference scheme, for example:

$$\left(\frac{\partial U^*F}{\delta x}\right)_{i,j}=\frac{1}{4\Delta x}[(U^*_{i+1,j}+U^*_{i,j})(F_{i+1,j}+F_{i,j})-(U^*_{i,j}+U^*_{i-1,j})(F_{i,j}+F_{i-1,j})], \tag{16}$$

and another one-sided spacial difference scheme on the boundary, for example:

$$\left(\frac{\partial U^*F}{\delta x}\right)_{I,j}=\frac{1}{2\Delta x}[4U^*_{I,j}F_{I,j}-(U^*_{I,j}+U^*_{I-1,j})(F_{I,j}+F_{I-1,j})], \tag{17}$$

where

$$1\leqslant i\leqslant I,\quad 1\leqslant j\leqslant J,\quad 1\leqslant k\leqslant K.$$

The forward time difference is used as follows:

$$\frac{\delta_t^+F}{\delta t}=\frac{F_{t+\delta t}-F_t}{\delta t}.$$

The foregoing primitive equations are written in ζ coordinate originally. The atmosphere is divided into six levels of ζ corresponding to 100, 300, 500, 700, 850, and 1000 hPa respectively. Because the vertical interval of every layer is not the same in ζ coordinate, we introduce a π coordinate in which the vertical intervals between any two adjacent levels are equal. They may be noted as follows:

$\pi=0$ at $P=100$ hPa,

$\pi=1$ at $P=1000$ hPa,

$$\pi'_{k+\frac{1}{2}}=\frac{\delta\pi}{\zeta_{k+1}-\zeta_k},$$

$$\pi'_{\frac{1}{2}}=\frac{\delta\pi}{\zeta_1},$$

$$\pi'_{K-\frac{1}{2}}=\frac{\delta\pi}{1-\zeta_{K-1}}.$$

We adopt a square forecast area containing 37×37 grid points and square meshes in a polar stereographic projection map. Let δx, δy and δt be the space steps and time step, respectively. Both δx and δy are equal to 540 km and δt is equal to 20 seconds.

2. *Adaptability Difference Scheme*

α and β, in Eqs. (1)—(4), are referred to as adaptability factors, so the foregoing difference equations are also called adaptability scheme. In this paper, α and β are equal to 1. With α and β other than 1, we may obtain various adaptability schemes. Thus, they may be used to adjust the moving velocity of systems (adjusting α) and the influence of the inertial gravity waves on the development process (adjusting β). It may also be used to construct a split model. When $\kappa=0$, it is the nondivergence approximate model. We may demonstrate that the foregoing difference scheme is in accordance with the rule of "generalized energy conservation".

III. THE ADVECTIVE DIFFERENCE SCHEME OF SIX-LEVEL PRIMITIVE EQUATIONS AND ITS SPLIT METHOD (MODEL 2)

It is time consuming to solve Eqs. (1)—(6) with the iteration model. In order to save computational time, we use a split method. The difference equations are as follows:

$$\left(\frac{\delta_t^+ u}{\delta t}\right)_{i,j,k} + \alpha D_{i,j,k}(\mathbf{w}^* \bar{u}) = \beta(-\bar{G}_x^{**} + \bar{f}^* \bar{v}^{**})_{i,j,k} + F_u, \tag{18}$$

$$\left(\frac{\delta_t^+ v}{\delta t}\right)_{i,j,k} + \alpha D_{i,j,k}(\mathbf{w}^* \bar{v}) = \beta(-\bar{G}_y^{**} - \bar{f}^* \bar{u}^{**})_{i,j,k} + F_v, \tag{19}$$

$$c_p\left(\frac{\delta_t^+ T}{\delta t}\right)_{i,j,k} + \alpha D_{i,j,k}(\mathbf{w}^* c_p \bar{T}) = \beta\Big[-D_{i,j,k}(\mathbf{w}^* \bar{\phi}^{**})$$
$$-k\left(\frac{\pi_k'}{P_{es}^*}\zeta\frac{\partial\bar{\phi}}{\partial\pi}\frac{\delta_t^+ P_{es}^*}{\delta t}\right) + \bar{G}_x^{**}\bar{u}^{**} + \bar{G}_y^{**}\bar{v}^{**}\Big]_{i,j,k} + F_T, \tag{20}$$

$$\kappa\left(\frac{\delta_t^+ P_{es}^*}{\delta t}\right)_{i,j} = -\sum_{k=1}^{K} \varepsilon_k \left(\frac{1}{\pi'}\right)_k \delta\pi (MN)_{i,j}\left[\frac{\delta_x U^*}{\delta x} + \frac{\delta_y V^*}{\delta y}\right]_{i,j,k}, \tag{21}$$

$$\begin{cases} w^*_{i,j,k+1} - w^*_{i,j,k} = -\left(\dfrac{\delta\pi}{\pi'}\right)_{k+\frac{1}{2}}\Bigg\{\kappa\left(\dfrac{\delta_t^+ P_{es}^*}{\delta t}\right)_{i,j} \\ \quad + \dfrac{1}{2}(M,N)_{i,j}\left[\left(\dfrac{\partial_x U^*}{\partial x} + \dfrac{\partial_y V^*}{\partial y}\right)_{i,j,k+1}\right. \\ \quad \left. + \left(\dfrac{\partial_x U^*}{\partial x} + \dfrac{\partial_y V^*}{\partial y}\right)_{i,j,k}\right]\Bigg\}, \\ w^*_{i,j,1} = 0, \end{cases} \tag{22}$$

$$\begin{cases} \phi_{i,j,k-1} - \phi_{i,j,k} = \dfrac{R}{2}[T_{i,j,k} + T_{i,j,k-1}]\ln\left(\dfrac{\zeta_k + P_t/P_{es}}{\zeta_{k-1} + P_t/P_{es}}\right)_{i,j}, \\ \phi_{i,j,K} = (\phi_\zeta^{**})_{i,j}. \end{cases} \tag{23}$$

In the foregoing equations, the terms containing α are the advective terms which represent development process, and the terms containing β represent adjustment process.

Marchuk and Zeng have shown that the adjustment process is rapid, and the development process is slow[6]. These two processes may be different from each other in physical property and time scale. The interaction between them is slight in short duration, and may be neglected. Therefore, we consider neither the term containing β in the computation of the advective term, nor the term containing α in the computation of the adjustment term. Because the representative time of these two processes is different, we may use different time step. As a consequence, it takes us much less computing time. Some of the notations in the Eqs. (18)—(23) are as follows:

$$D_{i,j,k}(w^*F)=M_{i,j}\left[\bar{u}^*\frac{\partial_x\bar{F}}{\partial x}+\bar{v}^*\frac{\partial_y\bar{F}}{\partial y}+\frac{\pi' w^*}{P^*_{es}}\frac{\partial_\pi\bar{F}}{\partial\pi}\right]_{i,j,k},$$

$$\bar{G}^{**}_x=M_{i,j}\left(\frac{\partial_x\bar{\phi}^{**}}{\partial x}+\frac{R\bar{T}^{**}_e}{P^*_{es}}\cdot\frac{\partial\bar{P}^*_{es}}{\partial x}\right)_{i,j,k},$$

$$\bar{T}^{**}_e=\frac{\zeta}{\zeta+P_t/P^{**}_{es}}\bar{T}^{**}.$$

The other expressions are the same as those mentioned in section II.

IV. INITIALIZATION AND BOUNDARY CONDITION

1. *Initialization*

For simplicity, the initial conditions used in this paper are geostrophic winds calculated from the pressure-height analyses.

The initial temperatures are calculated with the following static equations:

$$T_{i,j,k}=-\frac{1}{R}\left(\frac{\partial\phi}{\partial\ln P}\right)_{i,j,k},$$

$$T_{i,j,1}=T_{i,j,2},$$

$$T_{i,j,K}=2T_{i,j,K-1}-T_{i,j,K-2}.$$

2. *Boundary Condition*

For the horizontal boundary condition, the normal velocity components are assumed to be zero. At the earth surface and the top of the atmosphere, the vertical velocity w vanishes. They are expressed as follows:

$$u_{1,j,k}=u_{I,j,k}=0,$$

$$v_{i,1,k}=v_{i,J,k}=0,$$

$$w_{i,j,1}=w_{i,j,K}=0,$$

$$\phi_{i,j,K}=(\phi^{**}_s)_{i,j}.$$

If we do not take the orography effect into consideration, $\phi_{i,j,k}$ is identically zero.

V. RESULTS OF NUMERICAL FORECAST

In this section, some examples of forecast are presented using an idealized initial field and the synoptic map as the initial data, respectively.

1. *Forecasting Result with an Idealized Initial Field*

In order to test the stability of this model, we construct a simple idealized field and make weather forecasting.

At first, we construct the initial temperature field at the six levels using the following formulas:

$$T(x,y,p)=\overline{T}(p)+T'(x,y,p)+T''(x,y,p),$$

$$\begin{cases} T'(x,y,p)=-A_1e^{-R^2/B_1} & (R<a), \\ T'(x,y,p)=0 & (R\geqslant a), \end{cases}$$

$$\begin{cases} T''(x,y,p)=-A_2e^{-R'^2/B_2} & (R'<b), \\ T''(x,y,p)=0 & (R'\geqslant b), \end{cases}$$

where $\overline{T}$ (p) is the function of pressure, R is the distance from the computed point to North Pole and R' is the distance from the computed point to the specified point. A_1, A_2, B_1, B_2, a and b are all constants, which are based on the center intensity of the idealized field, the intensity of disturbance and the position of the disturbance center. Then the idealized height field may be determined from the foregoing idealized temperature by means of static equation.

It is obvious that the manufactured temperature-pressure field is a polar vortex with its center not in the pole. Fig. 1 shows the idealized height of 500 hPa. We make weather forecast with the iterated method described in section II. A 5-day stable outout is obtained using this idealized initial field.

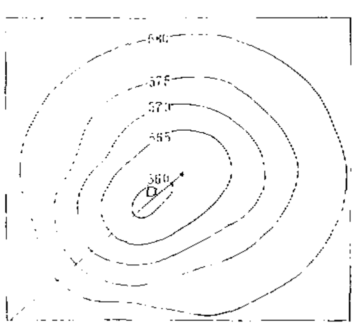

Fig. 1. 500 hPa analysis of idealized field.

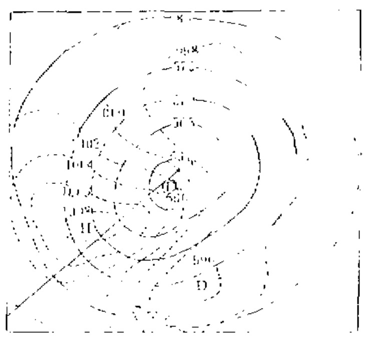

Fig. 2. 5-day 500 hPa forecast with model 1 (solid line), and 5 day surface pressure forecast (dashed line) with model 1.

Now let us analyse the 5-day forecast result.

In the initial chart, there is only a trough in the Northern Hemisphere. During the forecast course, we may find that the ultra-long wave draws back at first. Then, the trough begins to move eastward slowly. The developing process of the system of the other levels is the same as that of the 500 hPa. The trough moving velocity of all levels is different. The initial surface pressure is 1000 hPa everywhere, but on the fifth day there is a cyclogenesis before the trough-line of 500 hPa and an anticyclogenesis behind that, respectively, as shown in Fig. 2.

It may be seen from the foregoing rsult that the systems change reasonably and the computation is stable, so that we may draw a conclusion that this model is available.

2. *Forecasting Result with Nonlinear Iterational Difference Scheme (Model 1) for the Synoptic Chart*

In order to check the capability of the model and stability of computation, we should use the synoptic chart as the initial field and make forecast. Figs. 3—6 are 48 h 500 hPa height forecast and 24 h surface pressure forecast from the initial conditions at 12 Z, 28 July 1976 Chart with the model described in section Ⅱ. On the initial chart (Fig. 3) there are four major ridges right in the west part of the Pacific Ocean, in the west part of Northern United States, over Ural Mountains and over the Atlantic Ocean, and four major troughs in the west part of Europe, the east of Ural Mountains, the south-west part of Greenland and over the Central Pacific Ocean. These ridges are weak. The northern part of the trough over Europe is connected with the trough over the Central Pacific Ocean via Novaya Zemlya Island. Therefore, the ridge dominates North Pole. Fig. 4 shows 48 h forecast of 500 hPa (solid line) and verifying analysis(dashed line). The forecast result is that all the major forecast ridge-trough systems dominating Northern Hemisphere are stationary, and the

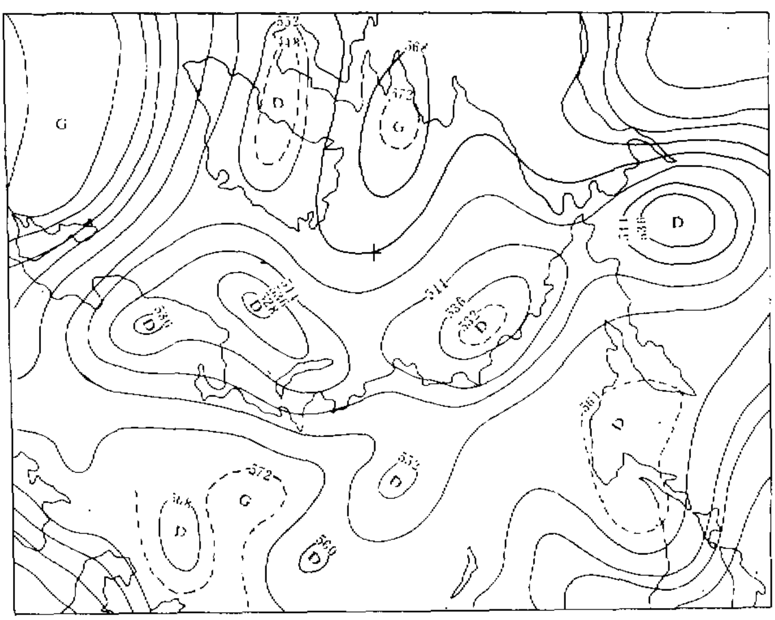

Fig. 3. 500 hPa analysis for 12 Z, 28 July 1976.

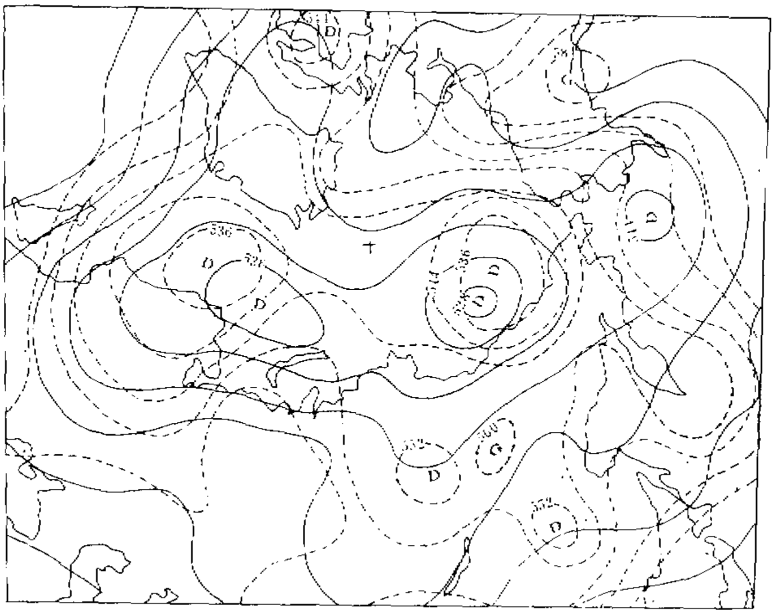

Fig. 4. 48 h 500 hPa forecast with model 1 (solid line), verifying at 12 Z, 30 July 1976 and 500 hPa analyzsis for 12 Z, 30 July 1976 (dashed line).

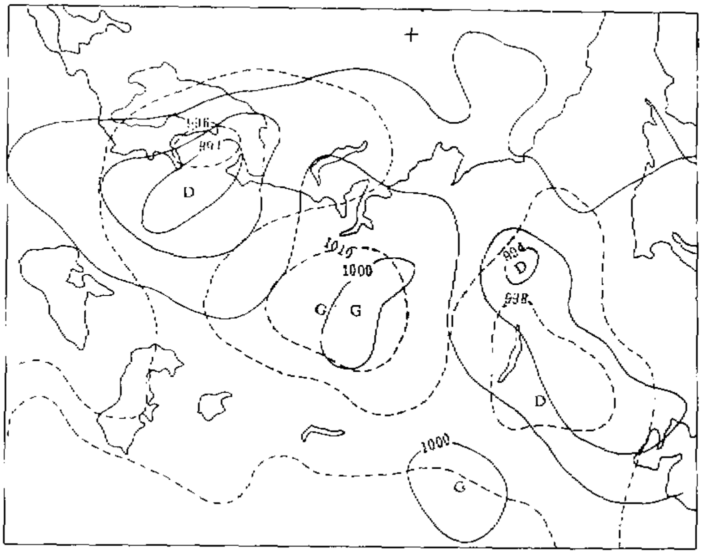

Fig. 5. 24 h surface pressure forecast with model 1, verifying at 12 Z, 29 July 1976 when $p=1000$ hPa (solid line), and actual pressure (dashed line), respectively.

intensification of the systems changes slightly. The 48 h forecast of 500 hPa is compared with the verifying chart. This forecast result is quite accurate. Individual system forecasted is weakened merely, but, in fact, it vanishes. For example, the center of depression east of Kamtchaka vanishes, but the forecasting result is weakened.

The initial surface pressure is supposed to be 1000 hPa everywhere. The surface pressure systems are substantially simulated 24 h later. Fig. 5 (solid line) shows the 24 h surface forecast which is the central pressure of 996 hPa for the cyclone in the west part of Europe, the central pressure of 994 hPa for the cyclone to the east of Lake Baikal and the central pressure of 1000 hPa for the anticyclone to the west of Lake Baikal. The distributions of these systems are in agreement with the observation (Fig. 6), but the forecast does not produce adequate intensification.

In order to test the effect of the initial surface condition, another forecast is made. The observed surface pressure at 12 Z, 28 July 1976 is used as initial condition. Fig. 5 (dashed line) shows the 24 h result. It is compared with the verifying chart shown in Fig. 6. This forecast is a little better than foregoing one. Therefore, we had better use the actual initial surface condition for short range forecast.

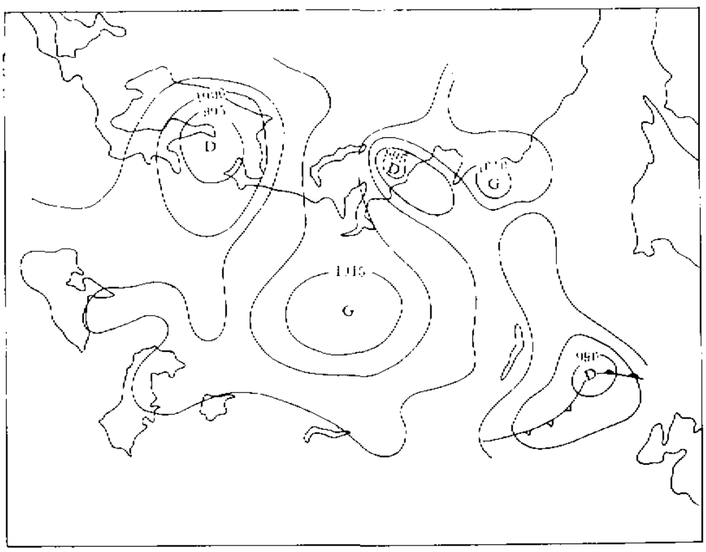

Fig. 6. Surface pressure analysis for 12 Z, 29 July 1976.

3. *Forecasting Result from the Split Scheme*

A forecast is made from the idealized initial condition described in this paper with split method. The result is as good as the foregoing one mentioned in subsection V. 2. It is not discussed here.

In order to understand the forecast effect with the foregoing two models, the same actual case is used. Fig. 7 shows the 48 h forecast from the initial conditions at 12 Z, 28

July 1976 chart with split method. The major forecasting ridge-trough systems dominating Northern Hemisphere are stationary too, so that the forecast result is as good as the previous one which is forecasted with model 1. However, the computational velocity with split method is much quicker than model 1. Therefore, we think that the split scheme is available.

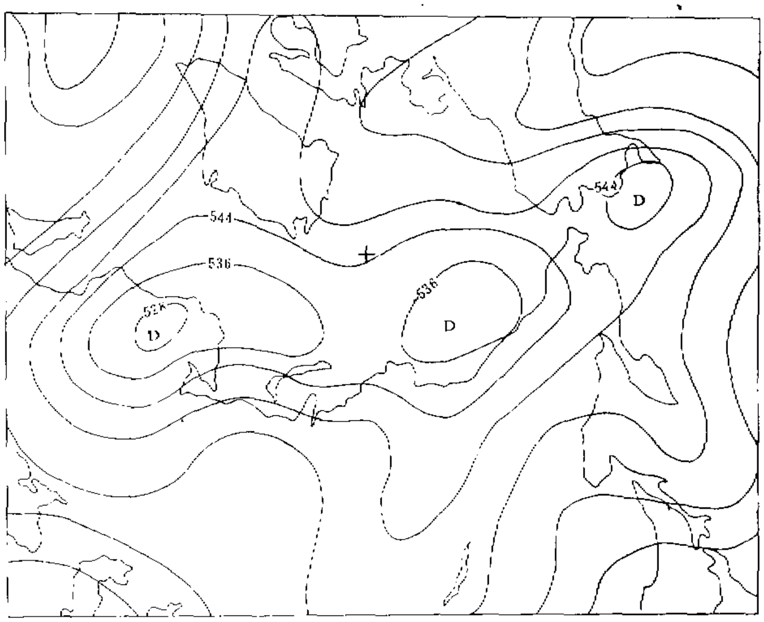

Fig. 7. 48 h 500 hPa forecast with model 2, verifying at 12 Z, 30 July 1976.

VI. CONCLUSION

An adaptability difference scheme of six-level primitive equations is used. The forecast results are successful. In order to save the computational time, we use split method again and get satisfactory result too.

In this paper, we only introduce a stable case. We have forecasted other cases about cold wave. They are satisfactory too.

In our work, the difference mesh is too large. It may affect the forecast result. Besides, this model does not contain heat source and orograph. We shall take those factors into account in successive work.

REFERENCES

[1] 曾庆存，二层模式的完整流体力学方程组在短期天气预报中的应用，动力气象论文集 (二),科学出版社, *1963, 133—152.*

[2] 刘瑞芝、张济朋，正压原始方程的一个数值试验，气象学报，**35**(1965),1： 75—81.

[3] 曾庆存、季仲贞、袁重光,原始方程差分格式的设计，第二次全国数值天气预报会议论文集，1980, 300—313.

[4] 朱抱真等，一个包括地形和非绝热作用的原始方程数值模式，气象学报，**38**(1980),2： 97—105.

[5] 黄荣辉、李荣凤，大气气温和风场垂直分布的统计特征及其在设计数值天气预报模式中的应用，大气科学, **5**(1981),3： 300—309.

[6] 曾庆存，大气中的适应过程和发展过程 (一),气象学报，**33**(1963),2: 163—174.